

Oscillations of the fusion cross-sections in the $^{16}\text{O}+^{16}\text{O}$ reaction

M V CHUSHNYAKOVA^{1,2,*} and I I GONTCHAR³

¹Physics Department, Omsk State Technical University, Omsk, Russia

²Physics and Chemistry Department, Omsk State Transport University, Omsk, Russia

³Department of Applied Physics, Tomsk Polytechnic University, Tomsk, Russia

*Corresponding author. E-mail: maria.chushnyakova@gmail.com

MS received 9 May 2014; revised 7 August 2014; accepted 21 August 2014

DOI: 10.1007/s12043-014-0917-0; ePublication: 27 June 2015

Abstract. Evolution of the fusion cross-section in the $^{16}\text{O}+^{16}\text{O}$ reaction has been analysed. It is shown, both analytically and numerically, that in this excitation function some oscillations can be observed. These oscillations are related to the quantum character of the orbital angular momentum increase as well as to the distinct features of the $^{16}\text{O}+^{16}\text{O}$ reaction. In order to perform the numerical calculations, the fluctuation–dissipation model and the single barrier penetration model are used. It turns out that the experimental data available in the literature do not have any definite proof about the presence or absence of the oscillations. We stress, that the question still remains unanswered for more than three decades whereas during this time lapse the experimental errors for other reactions are reduced to 1–2%.

Keywords. Heavy-ion fusion; fluctuation–dissipation dynamics; barrier penetration model; double-folding M3Y potential.

PACS Nos 25.70.Jj; 25.60.Pj; 24.10.–i

1. Introduction

Majority of our knowledge on the structure of atomic nuclei is obtained by studying the nucleus–nucleus collisions. Such collisions often result in direct reactions (e.g., transfer of nucleons) or in the orbital motion which can lead to the formation of compound nucleus (fusion) or quasifission [1,2]. In this paper we are interested in the collision of light nuclei at energies well above the Coulomb barrier, when the capture into orbital motion always results in fusion. Experimental fusion cross-section at the collision energy exceeding the Coulomb barrier usually increases monotonically, reaches a maximum and then decreases [3,4].

The theoretical fusion cross-section is calculated using the standard quantum-mechanical formula

$$\sigma = \frac{\pi \hbar^2}{2m_R E_{c.m.}} \sum_{L=0}^{L_c} (2L + 1) T_L, \quad (1)$$

where $m_R = m_n A_P A_T / (A_P + A_T)$ is the reduced mass; L_c denotes the value of the orbital angular momentum (in units of \hbar) at which the transmission coefficient T_L becomes zero with the required accuracy; m_n stands for the nucleon mass; A_P and A_T are the mass numbers of the projectile (P) and target (T) nuclei, respectively; $E_{c.m.}$ is the collision energy in the centre-of-mass frame. As the angular momentum is quantized, its value increases by $\Delta L = 2$ provided the colliding nuclei are identical and have zero spin, and by $\Delta L = 1$ in all other cases [5].

As $E_{c.m.}$ increases, at the given value of L , the transmission coefficient gradually increases from 0 to 1. In addition, the value of L_c also increases. However, the multiplier in front of the summation in eq. (1) decreases with $E_{c.m.}$ due to the decrease of the de Broglie wavelength. Thus, one can expect the theoretical excitation function $\sigma(E_{c.m.})$ to behave non-monotonically subject of the manner of the increase in L_c and T_L .

In our previous work [6], the fusion excitation function in the $^{16}\text{O}+^{16}\text{O}$ reaction at energies $U_{B0} < E_{c.m.} < 2U_{B0}$ has been analysed using the trajectory model with surface friction (TMSF) (U_{B0} is the s-wave barrier height). Within the framework of this model, the heavy-ion collision process is described by applying the stochastic dynamical equations of the Langevin type, in which the dissipation, thermal fluctuations, and memory effects are accounted for. The friction force is assumed to be proportional to the squared derivative of the strong nucleus–nucleus interaction potential. The latter is calculated within the framework of the double folding model with the density-dependent M3Y NN -forces possessing the finite-range exchange term (see detailed description of the model in [7,8]). It turns out that the calculated excitation function is very sensitive to the diffuseness of the nuclear matter density distribution and rather insensitive to the dynamics of the collision process, namely to the strength of the radial friction.

An alternative (and in fact more often used) way of theoretical analysis of the fusion data under consideration is the single barrier penetration model (BPM) which accounts for the quantum fluctuations but totally ignores thermal fluctuations [9–12]. Usually this model is applied in its simplest versions being either Hill–Wheeler formula for the parabolic barrier [13] or its consequence under additional approximations, the Wong formula [14].

The Hill–Wheeler formula for the transmission coefficient reads as

$$T_L = \left\{ 1 + \exp \left[2\pi(U_{BL} - E_{c.m.}) / (\hbar\omega_{BL}) \right] \right\}^{-1}, \quad (2)$$

where U_{BL} and $\hbar\omega_{BL}$ are respectively the height and curvature of the potential barrier for the given L value. In this work, the main objective is to study the influence of barrier curvature on the shape of the fusion excitation function, $\sigma(E_{c.m.})$. Earlier this topic was briefly discussed in [12]. We are unaware of any other work where the possible non-monotonic behaviour of $\sigma(E_{c.m.})$ is studied systematically.

2. Qualitative analysis

Let us consider the simplest situation when $\omega_{\text{BL}} = 0$. Then the transmission coefficient takes only two values: $T_L = 0$ at $L < L_c$ (i.e., when $E_{\text{c.m.}} < U_{\text{BL}}$) and $T_L = 1$ otherwise. In this case, summing up in eq. (1) results in

$$\sigma = \frac{\pi \hbar^2}{2m_{\text{R}}E_{\text{c.m.}}} (L_c^2 + 2L_c + 1) \quad (3)$$

at $\Delta L = 1$ and

$$\sigma = \frac{\pi \hbar^2}{2m_{\text{R}}E_{\text{c.m.}}} (L_c^2 + 3L_c + 2) \quad (4)$$

at $\Delta L = 2$ [12].

Considering eqs (3), (4) one can see that, as $E_{\text{c.m.}}$ increases, the cross-section does not behave monotonically: it ascends up when L_c increases by ΔL_c and decreases smoothly when L_c stays constant. This behaviour is illustrated schematically in figure 1. The collision energy increment $\Delta E_{\text{c.m.}}$ resulting in the increase of L_c by ΔL_c as well as the amplitude of the cross-section oscillations $\Delta\sigma_{\text{d}}$ (decrease) and $\Delta\sigma_{\text{i}}$ (increase) can be estimated analytically.

Neglecting the dissipation and barrier shift due to the centrifugal energy we obtain from the energy conservation law:

$$L_c^2 = 2m_{\text{R}}(E_{\text{c.m.}} - U_{\text{B0}}) R_{\text{B0}}^2 \hbar^{-2}. \quad (5)$$

The maximum angular momentum L_c increases abruptly by ΔL_c when the collision energy increases by $\Delta E_{\text{c.m.}}$. Equation (5) shows that these two increments are related to each other as follows:

$$L_c \Delta L_c = \Delta E_{\text{c.m.}} m_{\text{R}} R_{\text{B0}}^2 \hbar^{-2}. \quad (6)$$

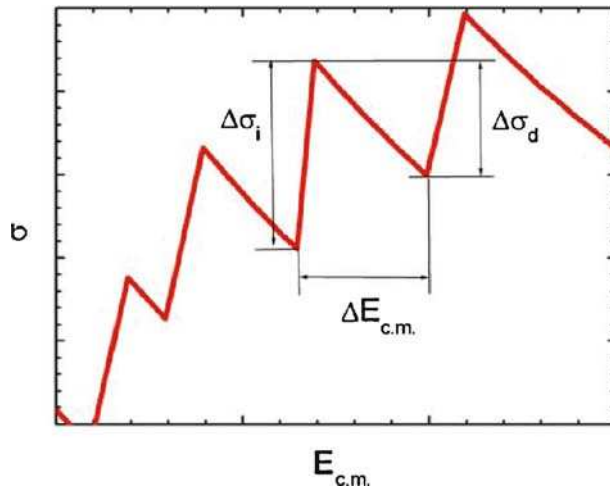


Figure 1. Schematic illustration of the oscillating fusion cross-section and the significance of $\Delta E_{\text{c.m.}}$, $\Delta\sigma_{\text{d}}$ and $\Delta\sigma_{\text{i}}$.

If $L_c > 10$, all the terms except L_c^2 in the brackets of eqs (3) and (4) can be neglected. Thus, the energy increment $\Delta E_{c.m.}$, during which the cross-section smoothly decreases by $\Delta\sigma_d$, reads as

$$\Delta E_{c.m.} = \frac{\hbar \Delta L_c}{R_{B0}} \sqrt{\frac{2(E_{c.m.} - U_{B0})}{m_R}}. \quad (7)$$

In order to derive a formula for $\Delta\sigma_d$ (considering the absolute value) one should find out a differential of eq. (3) or (4) keeping L_c constant. Applying eq. (7) we obtain

$$\Delta\sigma_d = \frac{\pi \hbar \Delta L_c R_{B0}}{E_{c.m.}} \left(1 - \frac{U_{B0}}{E_{c.m.}}\right) \sqrt{\frac{2(E_{c.m.} - U_{B0})}{m_R}}. \quad (8)$$

The increment $\Delta\sigma_i$ is found by taking a differential of eq. (3) or (4) as well but keeping the collision energy constant:

$$\Delta\sigma_i = \frac{\pi \hbar \Delta L_c R_{B0}}{E_{c.m.}} \sqrt{\frac{2(E_{c.m.} - U_{B0})}{m_R}}. \quad (9)$$

One can see that as $E_{c.m.}$ increases, the oscillations in the fusion cross-section related to the discrete character of the angular momentum can be observed with highest probability in the collision of identical light nuclei with spin zero: in this case R_{B0} and m_R are small and in addition $\Delta L_c = 2$. Consequently $\Delta E_{c.m.}$, $\Delta\sigma_d$ and $\Delta\sigma_i$ are relatively large. All these conditions are fulfilled for the $^{16}\text{O}+^{16}\text{O}$ reaction for which the excitation function was measured repeatedly [15–19].

3. The model for the quantitative analysis

In order to model the collision between spherical nuclei one needs to know the dependence of the nuclear, U_n , Coulomb, U_C , and centrifugal, U_L , parts of the interaction energy upon the center-of-mass distance R . For U_n the double folding model with the density-dependent M3Y NN -forces possessing the finite-range exchange term [20] is used. In this work, the dependencies $U_n(R)$ and $U_C(R)$ are calculated using the computer code DFMSPH published in [21]. The input parameter for the code is the distribution of the centers-of-mass of the nucleons at the ground state of the nuclei (which we shall refer to as ‘the density distribution’) [22]. Following [23], in this work for this distribution we use the Fermi–Dirac (or equivalently Woods–Saxon) profile whose half-density radius $R_0 = 2.525$ fm and diffuseness $a_0 = 0.45$ fm.

The value ω_{BL} needed for the BPM calculation reads

$$\omega_{BL} = \left| \frac{d^2 [U_n + U_C + U_L]}{m_R dR^2} \right|^{1/2}. \quad (10)$$

For dynamical simulation, the nuclear energy U_n calculated using the code DFMSPH is approximated by the Gross–Kalinowski profile (GK, see eqs (24) and (25) of [8]). The centrifugal energy is calculated as

$$U_L = \frac{\hbar^2 L^2}{2R^2 m_R}. \quad (11)$$

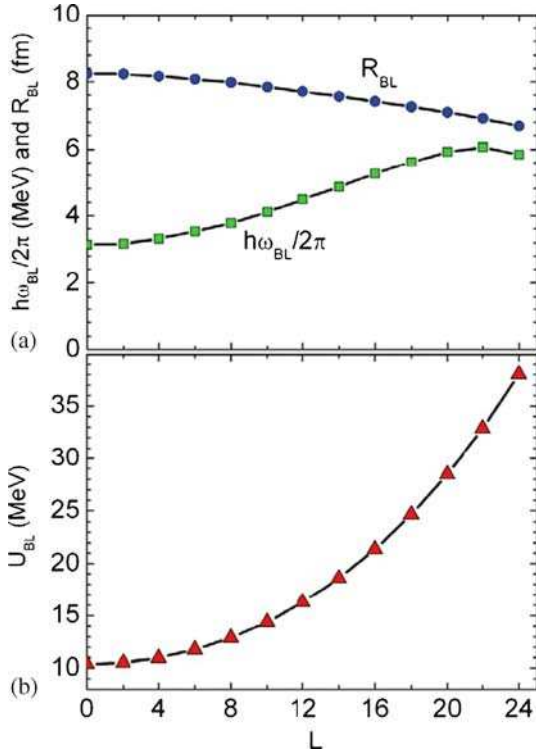


Figure 2. The Coulomb barrier parameters (radius R_{BL} and curvature $\hbar\omega_{BL}$ in **a**, height U_{BL} in **b**) vs. the angular momentum.

The fusion cross-section is calculated according to eq. (1); the transmission coefficient is calculated either using eq. (2) (BPM), or according to the dynamical routine described in [7] (TMSF). In the BPM calculation the barrier curvature $\hbar\omega_{BL}$ can be multiplied by a constant k .

In figure 2, the barrier parameters, namely the radius R_{BL} and the curvature $\hbar\omega_{BL}$ (figure 2a) and its height U_{BL} (figure 2b) are presented as functions of angular momentum. As L increases, the barrier becomes higher and its radius decreases due to the repulsive role of the centrifugal term in the effective potential. The value of $\hbar\omega_{BL}$ significantly increases with the angular momentum. Similar behaviour was demonstrated earlier in [24]. We shall see below that this increase of $\hbar\omega_{BL}$ might play some role in the appearance of the fusion cross-section oscillations.

4. Experimental data

In figure 3a, all the experimental fusion cross-sections for the $^{16}\text{O}+^{16}\text{O}$ reaction, available in the literature, are shown. First, we see that the data obtained by different groups do not agree with each other both at the energies near the barrier and also at higher energies. Second, in all experiments at $E_{c.m.} > 20$ MeV there seems to appear some oscillations.

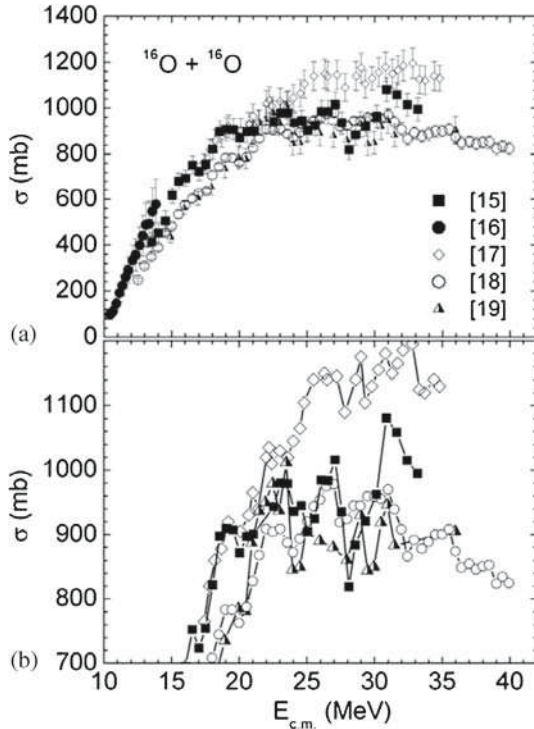


Figure 3. Experimental fusion excitation functions measured in [15–19] in different scales: (a) in general, with error bars and (b) the same data but in smaller range and without error bars. Some data points are taken from [25].

In order to show the oscillations clearly, the same data are displayed in figure 3b but without error bars and in the narrower cross-section range. Now one can conclude, as it is done in [12], that the cross-sections indeed oscillate. However, both the amplitudes and the periods of these oscillations are different in different experiments. It is regrettable that such contradiction in the data persists for the past thirty years, and the experimentalists do not pay attention to it. The errors in [15–19] are at best 5–7% and often reach 15%. Yet, during the last two decades the experimental errors for some other reactions have been reduced to 1–2% [9,26].

5. Results and discussion

In figure 4 the calculated fusion cross-sections are presented. In figure 4a results of the BPM calculations are presented where the barrier curvature artificially is made very small ($k = 0.05$). The cross-sections presented in figure 4b have been calculated within the framework of the dynamical model without fluctuations. Comparing these two curves one can see that the dynamical excitation function is somewhat suppressed and possesses the larger period of oscillations. Both these effects came from the frictional force and are more pronounced for larger $E_{c.m.}$.

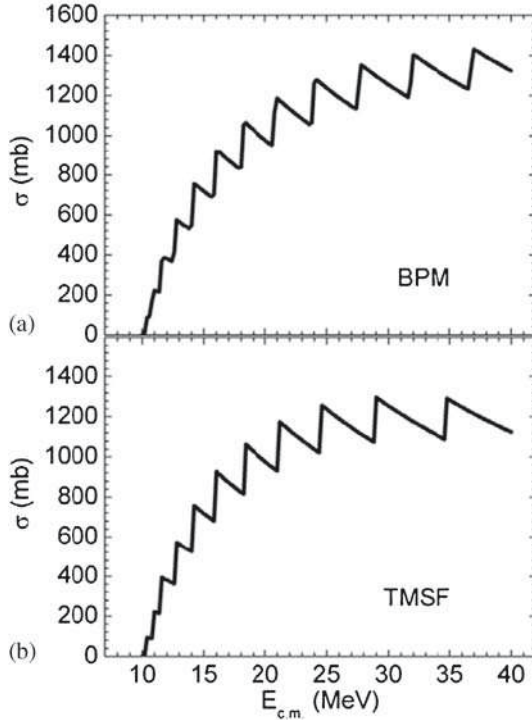


Figure 4. The fusion cross-sections calculated using (a) the BPM with the artificially reduced barrier curvature ($k = 0.05$) and (b) the dynamical approach without fluctuations with $K_R = 20 \text{ zs GeV}^{-1}$ ($1 \text{ zs} = 10^{-21} \text{ s}$).

According to eq. (7) the oscillation period $\Delta E_{c.m.}$ should increase as $E_{c.m.}$ increases. This is observed in both the curves of figure 4. Equation (8) implies that the amplitude of the cross-section decrease, $\Delta\sigma_d$, should increase with $E_{c.m.}$ until $E_{c.m.} = 4U_{B0}$. This is seen indeed in figure 4a. The amplitude of the cross-section increase, $\Delta\sigma_i$, according to eq. (9), should increase up to $E_{c.m.} = 2U_{B0}$ and then start decreasing. This is hardly seen in figure 4.

Let us now compare the values of $\Delta E_{c.m.}$, $\Delta\sigma_d$ and $\Delta\sigma_i$, obtained numerically within the BPM with the small barrier curvature (figure 4a) with those estimated using eqs (7)–(9). This comparison is presented in figure 5. In general, the numerical and approximate analytical values are in qualitative agreement, although the difference is sometimes significant. In particular even a flat maximum of $\Delta\sigma_i$ at $E_{c.m.} = 2U_{B0}$ is seen.

It seems that the sharp kinks as in figure 4 are never observed in the experiment. We see two reasons for that. First, the experimental errors are large and can mask the kinks. Second, the oscillations can be either smoothed or smeared out completely by the quantum and/or thermal fluctuations. These fluctuations in calculations of figure 4 have been artificially removed.

In order to observe the role of quantum fluctuations, the results of the calculations performed using the BPM with different values of barrier curvature ($k = 1.00, 0.60,$

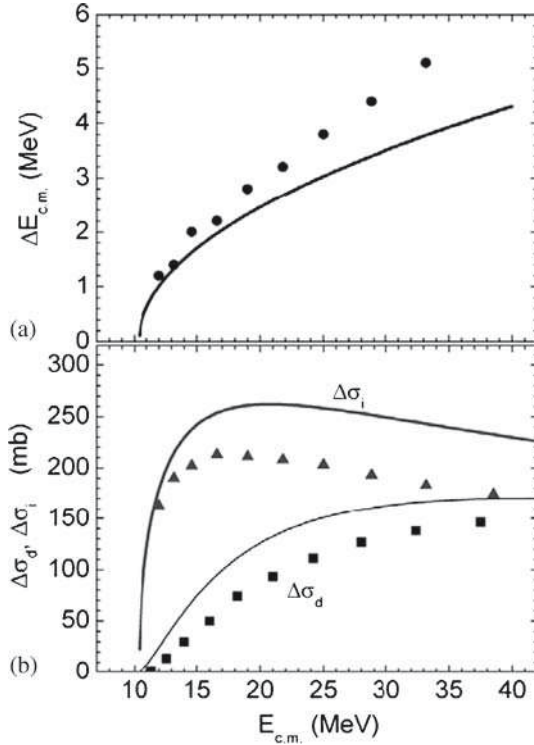


Figure 5. The values of $\Delta E_{c.m.}$ (a), $\Delta\sigma_d$ and $\Delta\sigma_i$ (b) obtained numerically within the BPM with the small barrier curvature (symbols) in comparison with those estimated using eqs (7)–(9) (curves) vs. the collision energy.

0.30) are presented in figure 6. Results corresponding to $k = 0.05$ which are presented in figure 4a are also displayed in figure 6.

In figure 6a only the results with $k = 1.00$ and 0.05 are presented. We see that the variation of the barrier curvature does not affect the average trend of $\sigma(E_{c.m.})$ but influences only the depth of the oscillations. In order to make this clear, in figure 6b all four calculated excitation functions are shown, each shifted up by 150 mb relatively to the previous one. It is clear now that the saw-tooth curve corresponding to $k = 0.05$ becomes softly oscillating at $k = 0.60$. At $k = 1.00$ the oscillations are almost invisible.

In order to examine this effect, let us consider figures 2a and 5a. In figure 2a we see that the typical value of the barrier curvature $\hbar\omega_{BL}$, which is the measure of smearing of T_L , is rather large: from 3 to 6 MeV. This is close to the cross-section oscillation period $\Delta E_{c.m.}$ in figure 5a and as a result the oscillations are almost totally erased in the curve corresponding to $k = 1.00$ in figure 6.

We compare our results with the experimental data of Fernandez *et al* [17] and Tserruya *et al* [15] in figures 7 and 8, respectively. The calculations were performed within the framework of the BPM ($k = 1$, label ‘0’) and of the TMSF with $K_R = 10$ zs GeV^{-1} (label ‘1’), 20 zs GeV^{-1} (label ‘2’) and 40 zs GeV^{-1} (label ‘4’). In the figures we see that the BPM overestimates both datasets. In figure 7 the TMSF calculations ‘4’ agree

Oscillations of the fusion cross-sections in the $^{16}\text{O}+^{16}\text{O}$ reaction

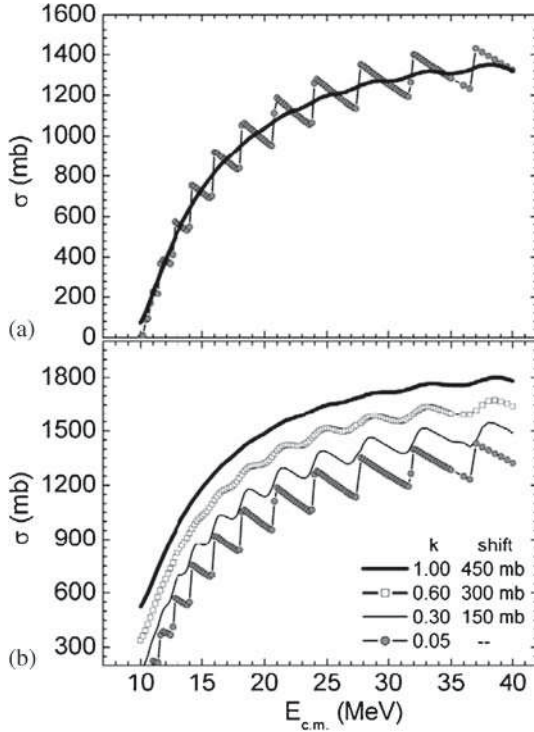


Figure 6. The fusion excitation functions calculated within the framework of the BPM with different values of k . In (a) only the results with $k = 1.00$ and 0.05 are presented. In (b) each curve is shifted up by 150 mb relatively to the previous one.

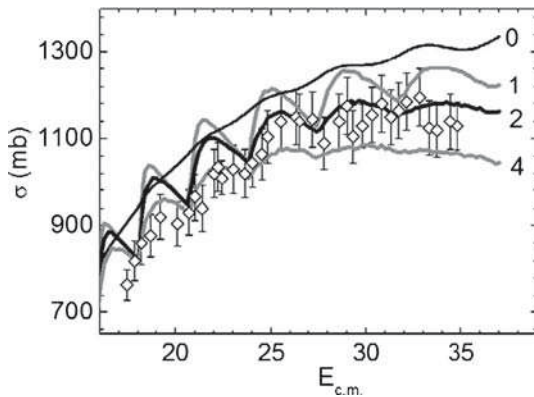


Figure 7. The experimental data of Fernandez *et al* [17] (symbols) in comparison with our calculations (lines) performed within the framework of the BPM ($k = 1$, label '0') and of the TMSF with $K_R = 10 \text{ zs GeV}^{-1}$ (label '1'), 20 zs GeV^{-1} (label '2') and 40 zs GeV^{-1} (label '4').

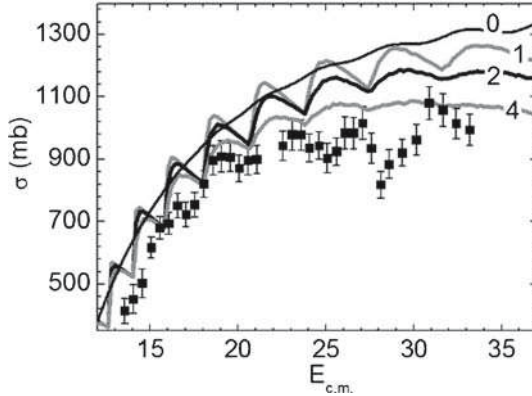


Figure 8. Same as figure 7, but with the experimental data of Tserruya *et al* [15].

with the data [17] for $E_{c.m.} < 25$ MeV. At higher collision energies, these data require smaller values of K_R : 20 zS GeV^{-1} seems to be convenient. No oscillations can be identified in the data of [17] due to large errors: these data are approximated by the equation

$$\sigma_{\text{appr}}(E_{c.m.}) = -734.3 + 122.3 \cdot E_{c.m.} - 1.98 \cdot E_{c.m.}^2. \quad (12)$$

The χ^2 of this approximation, calculated as

$$\chi^2 = \frac{1}{N} \sum \frac{(\sigma_{\text{appr}} - \sigma_{\text{exp}})^2}{\Delta\sigma_{\text{exp}}^2}, \quad (13)$$

is equal to 0.2.

In figure 8 the data of Tserruya *et al* [15] demonstrate the oscillations exceeding the experimental errors at energies around 25–35 MeV. The period of these oscillations is about 3–4 MeV which is compatible with our results ‘1’ and ‘2’. However, the absolute values of the calculated cross-sections are significantly above the data.

As the experimental data are very contradicting, we compare our results with those calculated within the framework of the TDHF in [12]. This method accounts for neither quantum nor thermal fluctuations and provides the transmission coefficient equal to either 0 or 1. Therefore, in [12] the Hill–Wheeler formula (eq. (2)) was used to smooth the kinks. For this aim the barrier height in eq. (2) was taken from the TDHF calculations and the curvature was taken to be equal to 2.5 MeV for all L . Results of the comparison are plotted in figure 9. In figures 9a and 9b, we present the results corresponding to the BPM and dynamical modelling, respectively. The curves without symbols represent results of [12] (same in both (a) and (b)). The excitation functions, which include fluctuations, are shifted up by 300 mb to help the reader.

We see in figure 9a that in general, our BPM calculations (which are extremely fast) result in good agreement with the very computer-time-consuming TDHF calculations. This is surprising keeping in mind that for these calculations we use the Fermi–Dirac density distribution. At higher energies there is some mismatch between the corresponding peak positions: the period of oscillations in our calculations becomes larger than

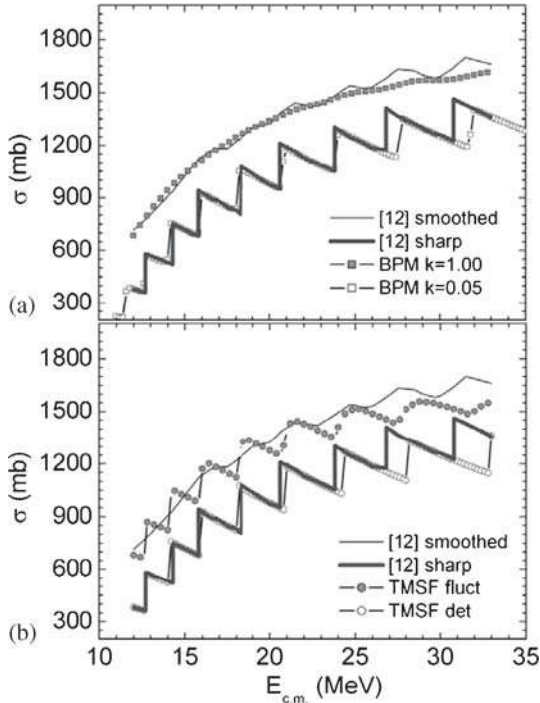


Figure 9. Our results (lines with symbols) are compared with the theoretical excitation functions taken from [12] (lines without symbols). Thick lines correspond to the original TDHF calculations of [12] whereas the thin lines represent the same calculations smoothed by using eq. (2), i.e., including quantum fluctuations. Curves with boxes correspond to our BPM calculations. Curves with circles represent the results of the dynamical calculations with the thermal fluctuations and without thermal fluctuations (solid and open circles, respectively). The excitation functions which include fluctuations are shifted up by 300 mb. (a) represents the results obtained within the BPM whereas (b) represents the results obtained within the TMSF.

in the TDHF calculations. Our guess is that the reason for this difference is the self-consistent accounting for the dynamical deformations of the colliding nuclei within the framework of the TDHF approach. These deformations are expected to become increasingly important at higher collision energies, i.e., at larger values of angular momentum. In our calculations, the deformations are ignored at all collision energies.

In figure 9b, the agreement of our dynamical calculations using $K_R = 10 \text{ zs GeV}^{-1}$ with the TDHF cross-sections is also good for the kinky curve, where neither in our calculations nor in the TDHF, the fluctuations are accounted for. However, at high energies, mismatch similar to the figure 9a is observed. Moreover, this mismatch starts earlier (at lower energies) and becomes more pronounced in comparison with the BPM case.

When fluctuations are included (upper curves in figure 9b) the agreement becomes poorer. This is probably due to the difference in nature of these fluctuations.

6. Conclusions

First, we have analysed all the available experimental data on the energy dependence of the fusion cross-section in $^{16}\text{O}+^{16}\text{O}$ reaction. This analysis has shown that the data of different groups are almost always in contradiction with each other. Moreover, the experimental errors are about 15%. Therefore, the statement of some experimental works, that in the fusion excitation function in this reaction oscillations are observed, is doubtful.

Second, we have shown both numerically and analytically that oscillations can be observed in this excitation function due to the quantized nature of the angular momentum and the distinct feature ($\Delta L = 2$) of this reaction. The fluctuation–dissipation model (TMSF) and the barrier penetration model (BPM) were used for numerical calculations. It turned out that both quantum and thermal fluctuations destroyed the oscillations. Unfortunately, we did not still succeed to unify both kinds of fluctuations within the same model.

Third, we have found that our calculations result in close agreement with the very computer-time-consuming TDHF calculations. This is probably because both the TDHF calculations (through the Skyrme forces) and our calculations (through the double-folding potential) use the parameters (although different ones) adjusted to reproduce the ground state charge distribution of ^{16}O .

Finally, results of the calculations and analysis of the experimental data demonstrate that nothing definite can be said about the absence or presence of oscillations. This question stays unresolved for more than three decades and we are not aware of any work which contains critical detailed discussion of the problem of oscillations. During these decades, the experimental errors of the fusion excitation functions for some other reactions were reduced to 1–2%. We hope to attract the attention of the experimentalists to this interesting problem.

Acknowledgements

MVC is grateful to the Dmitry Zimin Foundation ‘Dynasty’ for financial support.

References

- [1] Yu Ts Oganessian and Yu A Lazarev, *Heavy ions and nuclear fission (In Treatise on Heavy Ion Science)* edited by D A Bromley (Plenum Press, New York, 1985) Vol. 4, pp. 3–254
- [2] G G Adamian, N V Antonenko and W Scheid, *Phys. Rev. C* **68**, 034601 (2003)
- [3] D J Hinde, R J Charity, G S Foote, J R Leigh, J O Newton, S Ogaza and A Chatterjee, *Nucl. Phys. A* **452**, 550 (1986)
- [4] P Fröbrich, *Phys. Rep.* **116**, 337 (1984)
- [5] P Fröbrich and R Lipperheide, Theory of nuclear reactions, in: *Oxford studies in nuclear physics* (Oxford University Press, 1996) Vol. 18
- [6] M V Chushnyakova, I I Gontchar and S N Krokhin, *Commun. Omsk University* **4(70)**, 75 (2013)
- [7] M V Chushnyakova and I I Gontchar, *Phys. Rev. C* **87**, 014614 (2013)
- [8] M V Chushnyakova and I I Gontchar, *J. Phys. G* **40**, 095108 (2013)

Oscillations of the fusion cross-sections in the $^{16}\text{O}+^{16}\text{O}$ reaction

- [9] J O Newton, R D Butt, M Dasgupta, D J Hinde, I I Gontchar, C R Morton and K Hagino, *Phys. Rev. C* **70**, 024605 (2004)
- [10] M Rashdan, *J. Phys. G* **22**, 139 (1996)
- [11] H Esbensen, *Phys. Rev. C* **77**, 054608 (2008)
- [12] C Simenel, R Keser, A S Umar and V E Oberacker, *Phys. Rev. C* **88**, 024617 (2013)
- [13] D L Hill and J A Wheeler, *Phys. Rev.* **89**, 1102 (1953)
- [14] C Y Wong, *Phys. Rev. Lett.* **31**, 766 (1973)
- [15] I Tserruya, Y Eisen, D Pelte, A Gavron, H Oeschler, D Berndt and H L Harney, *Phys. Rev. C* **18**, 1688 (1978)
- [16] A Kuronen, J Keinonen and P Tikkanen, *Phys. Rev. C* **35**, 591 (1987)
- [17] B Fernandez, C Gaarde, J S Larsen, S Pontoppidan and F Videbaek, *Nucl. Phys. A* **306**, 259 (1978)
- [18] J J Kolata, R M Freeman, F Haas, B Heusch and A Gallmann, *Phys. Rev. C* **19**, 2237 (1979)
- [19] D G Kovar, D F Geesaman and T H Braid *et al.*, *Phys. Rev. C* **20**, 1305 (1979)
- [20] Dao T Khoa, G R Satchler and W von Oertzen, *Phys. Rev. C* **56**, 954 (1997)
- [21] I I Gontchar and M V Chushnyakova, *Comput. Phys. Comm.* **181**, 168 (2010)
- [22] G R Satchler and W G Love, *Phys. Rep.* **55**, 183 (1979)
- [23] M El-Azab Farid and G R Satchler, *Nucl. Phys. A* **438**, 525 (1985)
- [24] I I Gontchar, D J Hinde, M Dasgupta, C R Morton and J O Newton, *Phys. Rev. C* **73**, 034610 (2006)
- [25] <http://nr.v.jinr.ru/nrv/webnrv/fusion/reactions.php>
- [26] M Dasgupta, D J Hinde, N Rowley and A M Stefanini, *Ann. Rev. Nucl. Part. Sci.* **48**, 401 (1998)